Completely Inelastic Bouncing Ball on a Forced Plate

Chris Rodesney, Phillip Gray, Jacob Yunis, and Nitin Arora

School of Physics, Georgia Institute of Technology, Atlanta, Georgia 30332, USA

(Dated: 15 December 2011)

In this paper, we investigate the dynamics of a completely inelastic ball on a vertically vibrated plate. We construct a computational model using various forcing waveforms for the plate and generate associated bifurcation diagrams. The forcing functions used are a superposition of two sine waves with an integer ratio of frequencies. We then observe experimentally some of the predictions made by the model for the case of a single sine wave forcing function.

I. INTRODUCTION

The system of a ball bouncing completely inelastically on a vibrated platform has been the subject of numerous studies[1,2], and the case of a simple harmonically vibrated plate was completely resolved by Gilet et al[2]. The main mechanism for analyzing the motion is measuring the time of flight between successive impacts of the ball with an n-cycle corresponding to the ball having n unique flight times before repeating. For small forcing, Gilet et al found an alternating series of one and two cycles with a small region containing an infinity of bifurcations around control parameter $\Gamma \simeq 7.253378$.

We investigate the case of a plate vibrated according to a superposition of two sine waves with a frequency ratio c:

$$x_p(t) = A[\sin(\omega t) + \sin(c\omega t)] \qquad (1)$$

The ball can "take off" when the acceleration of the plate is less than the acceleration of gravity, $-g$:

$$\ddot{x}_p(t) = -A[\omega^2 \sin(\omega t) + c^2\omega^2 \sin(c\omega t)] \leq -g$$
$$\frac{A\omega^2}{g}[\sin(\omega t) + c^2 \sin(c\omega t)] \geq 1 \qquad (2)$$

At this point, we nondimensionalize the equations of motion via the characteristic time $1/\omega$ and length g/ω^2, where g is the acceleration due to gravity. This defines a phase $\varphi = \omega t$, a generalized position $\chi = x\omega^2/g$, and a reduced acceleration $\Gamma = A\omega^2/g$. This last parameter Γ is our other control parameter, the first being the frequency ratio c.

In this dimensionless Γ, φ, χ regime, the forcing function of the plate is

$$\chi_p(\varphi) = \Gamma(\sin(\varphi) + \sin(c\varphi)). \qquad (3)$$

The position of the ball relative to the

$$\chi_b(\varphi) = \Gamma[\sin(\varphi_0)+\sin(c\varphi_0)-\sin(\varphi)-\sin(c\varphi)]+\Gamma[\cos(\varphi_0)+c\cos(c\varphi_0)](\varphi-\varphi_0)-1/2(\varphi-\varphi_0)^2 \quad (4)$$

plate is given in Equation 4, where φ_0 is the phase of the ball at takeoff. The ball takes off when the following dimensionless equation is satisfied:

$$\Gamma[\sin(\varphi) + c^2\sin(c\varphi)] \geq 1 \quad (5)$$

The flight time is defined as $\tau \equiv \varphi_i - \varphi_0$. Our primary means of visualizing the dynamics is via bifurcation diagrams. We plot the times of flight versus control parameter Γ for our various c values. For comparison with our experimental data, the dimensional flight time (in seconds) is $T = \tau/\omega$.

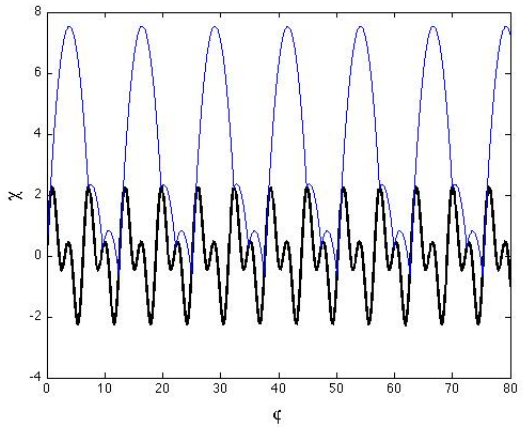

FIG. 1: Generalized position versus phase for $c = 2$, $\Gamma = 1.28$ case. Black is the motion of the plate and blue is the ball, which is constrained to remain above the plate.

The ball is able to land in two distinct regions; if the ball lands at a point when Eq. (5) is satisfied, it will immediately be launched back into the air. Otherwise, the ball will remain on the plate until Eq. (5) is satisfied. It is this second region that corresponds to a resetting of the ball, and often, the start of a new cycle. An interesting consequence of these two regions is the existence of a third region in the bifurcation plots, a forbidden zone[2] where certain times of flight cannot occur for a given Γ.

The case of $c = 1$ is a simple sine wave with amplitude 2Γ. This is identical (to a factor of 2) to the case studied by Gilet et al[2] and is used as a check for our computational model and experimental setup. The cases $c = 2$ and $c = 3$ are designed to elicit novel nonlinear behavior via a slightly more complicated system.

II. METHODS

Our experimental apparatus consists of a forced plate and rod assembly attached to a shaker with a 249.2 gram metal block as our ball. The ball is constrained to move along the rod in the vertical direction. A

computer outputs the forcing function to the plate through an amplifier, oscillating the rod and plate in the vertical direction. Embedded in the plate is an accelerometer, which is interfaced with a computer to record the acceleration of the plate. This allows us to check the reading from the accelerometer against the signal outputted to the plate, ensuring that they agree.

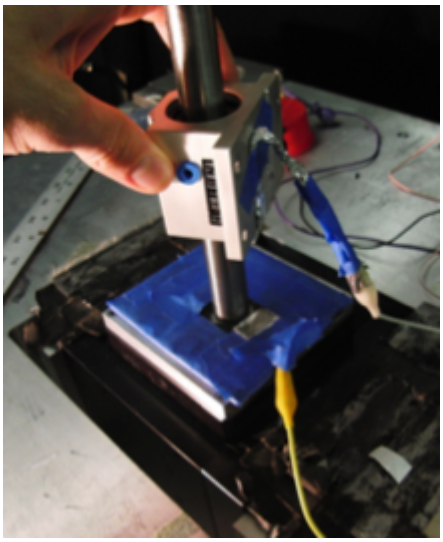

FIG. 2: Metal block on the rod and plate assembly. Note the wires coming from the continuity circuit.

In order to vary the control parameter Γ, we choose a fixed frequency between 20 Hz and 40 Hz and vary the amplitude. A relatively low frequency is chosen as a balance between maximizing flight times and also minimizing the magnitude of impacts of the ball on the plate, which cause unwanted feedback on the plate. We use a step function to ramp up the amplitude while pausing for a set number of cycles at each amplitude.

A portion of the plate is covered in a conducting material and integrated into a continuity circuit maintained at a constant 5 volts. The bottom of the ball is also covered in conducting material and connected to ground. In this way, the voltage in the circuit reads close to zero when the ball is in contact with the plate, and close to 5 volts when the ball is in the air. The voltage reading in the circuit is fed into a computer, along with the accelerometer reading, the original forcing function and a timestamp. Each of these is taken at a sampling rate of 20 kHz.

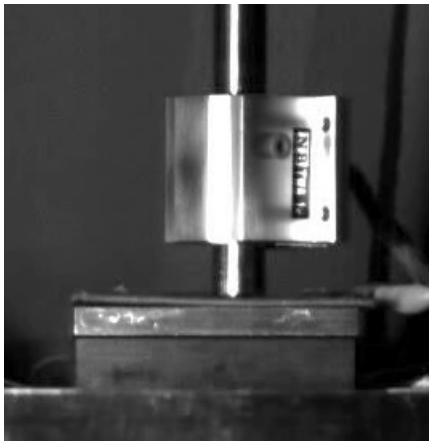

FIG. 3: Side view of the apparatus, used for video tracking.

We also sought to investigate what variables would make the system deviate from an ideal inelastic bouncing ball. Of course, the ball was is completely inelastic. There is also coulomb friction between the ball and the constraining rod, with the friction op-

posing the motion. These effects were analyzed by recording a drop of the ball using a high speed camera at 1000 frames per second, tracking the ball via imaging software and fitting the resultant motion to parabolic trajectories.

III. RESULTS

For the $c = 1$ case, bifurcation diagrams from our idealized computational model and one set of experimental data are shown in Figures 4 and 5 respectively. We note that because of the nature of the governing equation (Eq. 1), the Gamma values in the computational plot are 1/2 of those in the experimental plot.

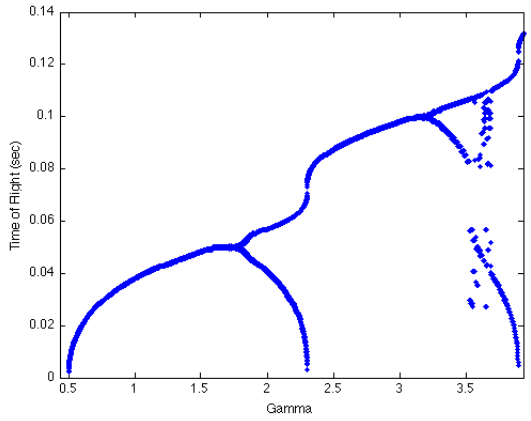

FIG. 4: Bifurcation diagram from the computational model. $c = 1$, $\omega = 20$.

We also notice that the experimental bifurcation diagram is in general much noisier than the computationally generated one.

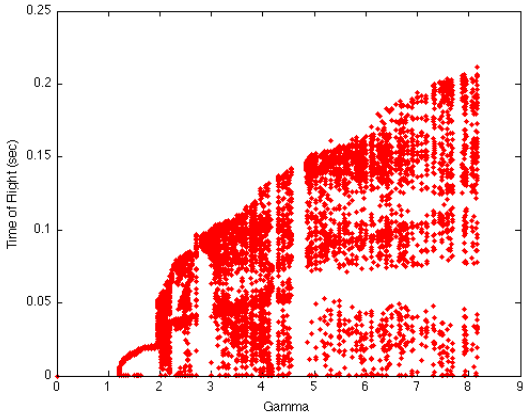

FIG. 5: Full bifurcation diagram from the experimental data. $c = 1$, $\omega = 20$.

The flight times very close to 0 stem from fast double-hits of the ball. These times are ignored as false flights from the continuity data. Despite this, it clearly displays a forbidden region around $T = 0.06s$ from $5 \leq \Gamma \leq 8$. A lobed shape is visible in the same region of Gamma for higher flight times, hinting at the existence of another forbidden region.

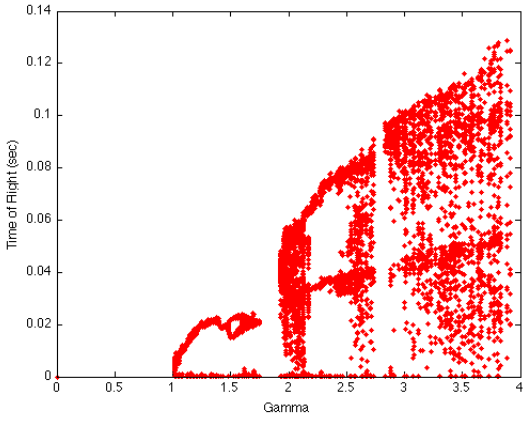

FIG. 6: Zoomed bifurcation diagram from the experimental data. $c = 1$, $\omega = 20$.

A slower sweep through the lower Gamma

values shown in Figure 6 reveals greater detail in the region of short flight times. This plot replicates the onset of a 1-cycle at $\Gamma = 1$ and steady increase in time of flight until a period-doubling bifurcation occurs around $\Gamma = 2$. Following this bifurcation is a short window of period 2 followed by the lobed appearance for higher Gamma values.

We implement a return map of T_n vs. T_{n+1} to analyze whether or not a periodic cycle exists for a given Gamma. For the one and two cycle regimes, the accompanying return maps in Figures 7 and 8 clearly illustrate periodicity. For chaotic behavior at higher Gamma values, the return map takes on a multimodal structure as illustrated by the bimodal example in Figure 9.

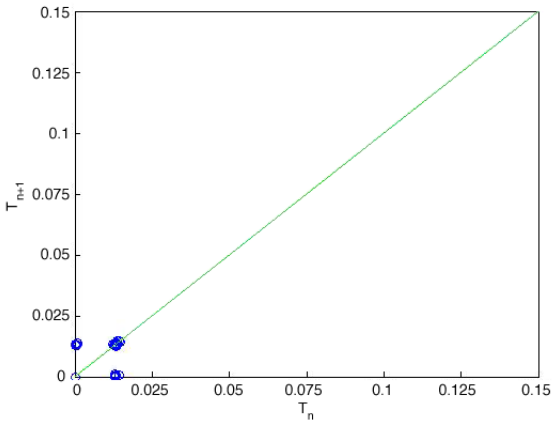

FIG. 7: Return map for a 1-cycle. $\Gamma = 1.2$

Bifurcation diagrams generated by our computational model for the $c = 2$ and $c = 3$ cases are presented in Figures 10 and 11 respectively. They exhibit the same growth

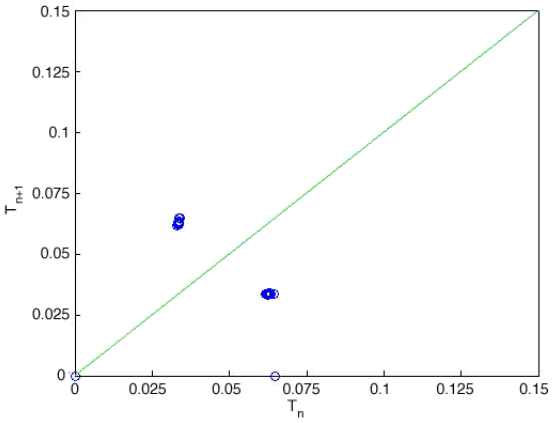

FIG. 8: Return map for a 2-cycle. $\Gamma = 2.25$

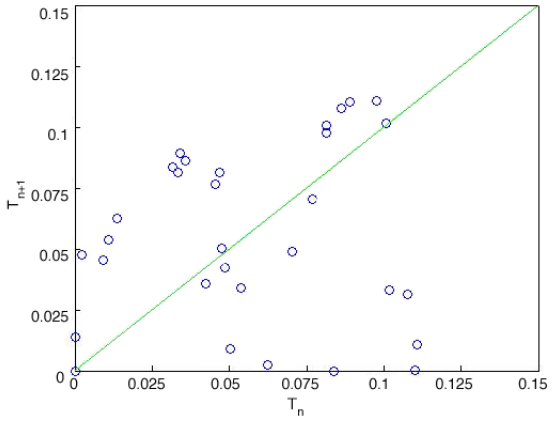

FIG. 9: Return map showing bimodal structure. $\Gamma = 3.4$

pattern for the maximum time of flight, and also contain the forbidden regions present in the simple harmonic case. However, they contain significantly more complexity than the $c = 1$ case.

IV. DISCUSSION

One error introduced into the data at higher Gamma values stems from a resonant

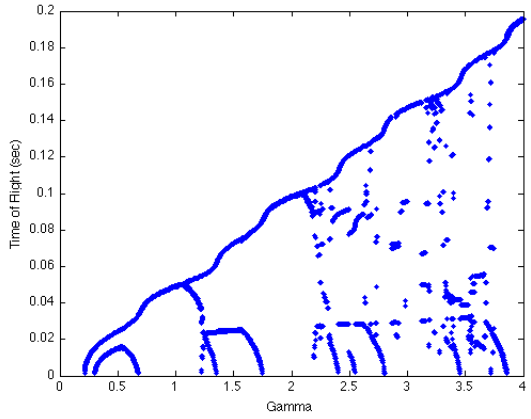

FIG. 10: Bifurcation diagram from the computational model. $c = 2$, $\omega = 20$.

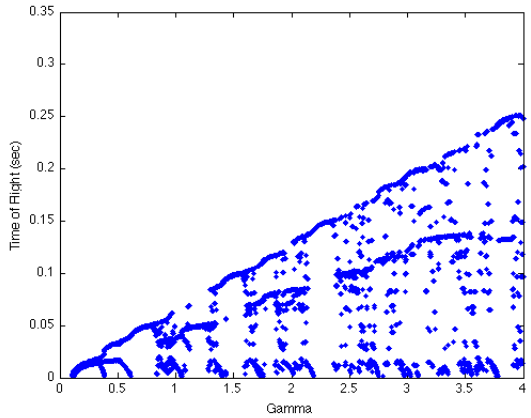

FIG. 11: Bifurcation diagram from the computational model. $c = 3$, $\omega = 20$.

oscillation of the plate due to feedback from the ball. For $\Gamma \geq 4$, the vertical displacements were sufficiently high for the repeated impacts of the ball to cause a resonant oscillation in the entire shaker and plate assembly. This oscillation was at a much lower frequency than the forcing frequency ω, but it was sufficiently large to perturb the periodic forcing of the plate. At large Gamma values, the motion of the plate was no longer true to the forcing function output by the computer.

As is evident in Figures 5 and 6, our experimentally determined times of flight for a 1-cycle are approximately 40% lower than expected from our computational model. Additionally, the onset of the first period doubling bifurcation occurs much sooner in our experimental data, at 58% of the expected value. The 2-cycle is also much more persistent. It remains through a much wider range of Gamma values than our computational model predicts.

Two sources of error not accounted for in our original model are Coulomb friction between the ball and the rod, and elasticity inherent in collisions between the ball and plate. Friction is taken to oppose the motion of the ball relative to the plate at approximately $0.3g$, and this effect is worked into a second, modified computational model. This modification brings the Gamma values at the first bifurcation into much better agreement with our experimental data, with the first bifurcation occurring at 83% of the expected computational value.

The other source of disagreement between the model and experimental data is the elasticity of the ball. The coefficient of restitution between the ball and the plate is 0.514 ± 0.02. In addition to causing "double-hits" with a very small time of flight, for a

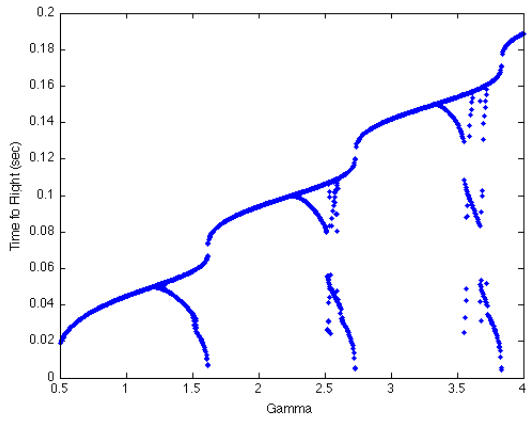

FIG. 12: Bifurcation diagram from the friction computational model. $c = 1$, $\omega = 20$.

sufficiently large displacement, the ball would bounce immediately on impact. This even occurs in the sticking region. This effect is a plausible explanation for the lack of 1-cycles for Gamma values larger than $\Gamma \approx 3$.

V. CONCLUSION

In conclusion, we experimentally recreate certain aspects of the completely inelastic ball on a harmonically forced plate. We observe the onset of bouncing, an initial period doubling bifurcation and a two-cycle. However the dynamics at higher Gamma values differ in our experiment, primarily due to elasticity and friction in the system. We also computationally model the behavior of a completely inelastic ball with a forcing function that is the superposition of two sine waves with integer multiple frequency.

In regard to future work, experimental investigation of the $c = 2$ and $c = 3$ cases is still to be done. Our experimental work in the $c = 1$ case was hampered by physical limitations, especially at higher Gamma values. These effects could be lessened using a less massive ball with a smaller coefficient of restitution. Additionally, further investigation into the bimodal structure found in the chaotic regions of the $c = 1$ case may lead to explanations of the system's dynamics.

REFERENCES

[1]A. Mehta and J. M. Luck, "Novel Temporal Behavior of a Nonlinear Dynamical System: The Completely Inelastic Bouncing Ball," Physical Review Letters **65**, 393 (1990).

[2]T. Gilet, N. Vandewalle, and S. Dorbolo, "Completely Inelastic Ball," Physical Review E **79**, 055201(R) (2009).